

ISSN 1029-8940 (Print)  
ISSN 2524-230X (Online)

UDC 591.478.7:598.279

<https://doi.org/10.29235/1029-8940-2021-66-2-232-246>

Received 16.12.2020

**Elena O. Fadeeva**

*A. N. Severtsov Institute of Ecology and Evolution of the Russian Academy of Sciences,  
Moscow, Russian Federation*

## **FEATURES OF THE ARCHITECTONICS OF THE MICROSTRUCTURE OF THE PRIMARY REMEX OF OWLS (STRIGIFORMES) DUE TO THE SPECIFICS OF THE FLIGHT**

**Abstract.** Conducted electron microscopic investigation of the primary remex fine structure of thirteen species of Owls (Strigiformes), using a scanning electron microscope (SEM). It is shown that Owls (Strigiformes) have a number of specific primary remex microstructural characteristics. First of all, these are the features of the structure of the pennaceous barb: a cross section configuration, a pith architectonics on the cross section and longitudinal sections, a cuticular structure of the barb.

A number of the unique features in the microstructure of the vanules of the pennaceous barb have been found for the first time (at the scanning electron microscope level, at a large SEM magnification). First of all, these are the structural features of the distal barbules and the structure of the apical portion of the barb with the elongated proximal barbules and the distal barbules tightly contiguous to the ramus and closed with each other. Mentioned characteristics make for the thick velvet-like dorsal surface of the vane and the presence of a complex of peculiar “bunches” (fringes) forming the cleft edge (a fringed edge) of the inner vane – exceptionally specific adaptive characteristics in Strigiformes.

Presented original research results suggest that Owls (Strigiformes) have a number specific microstructural characteristics of the primary remex and also a number of the unique features in the microstructure of the primary remex which reflecting the ecological and morphological adaptations conditioned by the flight specificity.

**Keywords:** Owls, electron microscopic investigation, primary remex, feather microstructure

**For citation:** Fadeeva E. O. Features of the architectonics of the microstructure of the primary remex of Owls (Strigiformes) due to the specifics of the flight. *Vesti Natsyonal'nai akademii navuk Belarusi. Seryya biyalagichnykh navuk = Proceedings of the National Academy of Sciences of Belarus. Biological series*, 2021, vol. 66, no. 2, pp. 232–246. <https://doi.org/10.29235/1029-8940-2021-66-2-232-246>

**Е. О. Фадеева**

*Институт проблем экологии и эволюции им. А. Н. Северцова РАН, Москва, Российская Федерация*

## **ОСОБЕННОСТИ АРХИТЕКТониКИ МИКРОСТРУКТУРЫ ПЕРВОСТЕПЕННОГО МАХОВОГО ПЕРА СОВООБРАЗНЫХ (STRIGIFORMES), ОБУСЛОВЛЕННЫЕ СПЕЦИФИКОЙ ПОЛЕТА**

**Аннотация.** Морфологические адаптации птиц, связанные со способностью к полету, достаточно подробно изучены. При этом практически не исследованным остается строение микроstructures пера, хотя именно микроструктурные характеристики играют важную роль в возникновении адаптационных эколого-морфологических особенностей архитектуры пера.

Совообразные (Strigiformes) – очень привлекательная для изучения группа птиц, с хорошо выраженными чертами специализации к ночному стилю охоты. Особый интерес вызывают комплексные исследования микроstructures пера Strigiformes с помощью сканирующего электронного микроскопа (SEM), что позволяет визуализировать тонкую морфологию пера.

В настоящей работе представлены оригинальные результаты сравнительного исследования (ранее никем не проводившегося) тонкого строения первостепенного махового пера 13 видов совообразных с использованием SEM. Данная работа – продолжение нашего исследования микроstructures контурного пера совообразных. Представленные результаты являются первой детальной информацией (на уровне SEM) о микроstructures первостепенного махового пера совообразных.

Установлено, что для совообразных характерен ряд специфических микроструктурных особенностей первостепенного махового пера. Прежде всего это особенности строения бородки первого порядка контурной части опахала пера: конфигурация поперечного среза, архитектура сердцевинки на поперечном и продольном срезах, строение кутикулы бородки. В работе представлены электросканограммы микроструктурных характеристик, приведены их основные морфометрические показатели. Впервые выявлены сугубо специфические адаптивные характеристики пера совообразных – уникальные особенности микроstructures опахальца бородки, обуславливающие густую ворсис-

стую дорсальную паверхнасць опахала і наяўнасць комплексу своеобразных «косіц», формуючых рассученны край унутранага опахала.

Выяўленыя спецыфічныя характарыстыкі тонкага строення пера першаснага маховага пера своеобразных могуць быць зроблены для вывучэння напраўленнасці і дынамікі складанай радыяцыі морфалагічных, у тым ліку адаптацыйных, змяненняў мікрасструктуры пера ў філагенезе птуц.

**Ключевые слова:** своеобразные, электронномикроскопическое исследование, першаснае маховае перо, мікрасструктура пера

**Для цитирования:** Фадеева, Е. О. Особенности архитектоники микроструктуры першаснага маховага пера своеобразных (Strigiformes), обусловленные спецификой полета / Е. О. Фадеева // Вест. Нац. акад. навук Беларусі. Сер. біял. навук. – 2021. – Т. 66, № 2. – С. 232–246 (на англ. яз.). <https://doi.org/10.29235/1029-8940-2021-66-2-232-246>

**Introduction.** Strigiformes are very interesting, in theoretical terms, groups of birds that are well separated morphologically and ecologically, combining common features with other birds of prey for a specific hunting style with a number of unique ecological and behavioral adaptations to the living conditions.

At present, the biology of the Strigiformes has been studied in some detail [1–12]. Nevertheless, in modern works that provide detailed descriptions of distinctive species-specific morphological features in the body structure and plumage of the Strigiformes [13–15], including an exhaustive description of the main aerodynamically advantageous macro-morphological characteristics of the contour feather of individual representatives of the Strigiformes [16–22], there is almost no information about microstructural features of the feather cover of the Strigiformes.

At the same time, the study of species-specific features of the feather architectonics and the identification of the main taxonomically important microstructural characteristics make it possible to effectively diagnose species by feathers and their fragments for the purposes of biological examination, as well as to reveal the specificity of the structure of feather elements, reflecting the birds' adaptation to living conditions, for example, enhancing the aerodynamic effect of the wing [18, 23–28].

In order to identify the main species-specific features of the fine structure of the feather of Strigiformes, as well as a number of microstructural characteristics of the feather, possibly having an adaptive nature, we first conducted a detailed comparative electron-microscopic investigation of the microstructure features of the primary remex of Strigiformes.

**Materials and research methods.** The objects of the study were adults of thirteen species of Strigiformes: Barn Owl *Tyto alba*, Eurasian Scops Owl *Otus scops*, Oriental Scops Owl *Otus sunia*, Snowy Owl *Nyctea scandiaca*, Eurasian Eagle-Owl *Bubo bubo*, Tawny Owl *Strix aluco*, Ural Owl *Strix uralensis*, Great Grey Owl *Strix nebulosa*, Northern Hawk-Owl *Surnia ulula*, Eurasian Pygmy Owl *Glaucidium passerinum*, Little Owl *Athene noctua*, Boreal Owl *Aegolius funereus*, Long-eared Owl *Asio otus*, which was a continuation of our study of the microstructural features of the contour feather of Strigiformes [25, 26, 29–31]. Species names and systematic order were given by Dickinson [32]. The terminology was used in accordance with the work of Lucas, Stettenheim [23].

The material for the work was the primary remiges, kindly provided to us by A. B. Savinetsky (A. N. Severtsov Institute of Ecology and Evolution of the Russian Academy of Sciences, Moscow), V. G. Babenko (Moscow State Pedagogical University), and P. I. Dudin (State Nature Reserve “Galichya Gora”).

For the comparative electron-microscopic investigation we used the most informative fragments of a feather: pennaceous barbs of a primary remex and pennaceous barbules of a primary remex (Fig. 1).

With separate copies for each of the studied species of Strigiformes, a comparative analysis was carried out using a method based on the selection of a row of barbs of a specific area of the vanes [34, 35]. A series of 10–15 pennaceous barbs of the primary remiges inner vane was used in one individual of each species. The identification of species-specific microstructural characteristics was carried out in four sections of each barb. At the same time, we included only those species-specific characteristics that were noted in the structure of each, without exception, barb of the selected row.

Thus, the data below are based on a detailed analysis of 40–60 sample sites in one individual of each studied species of Strigiformes.

Preparation of barbs was carried out according to the following method repeatedly approved by us [25–31, 36, 37].

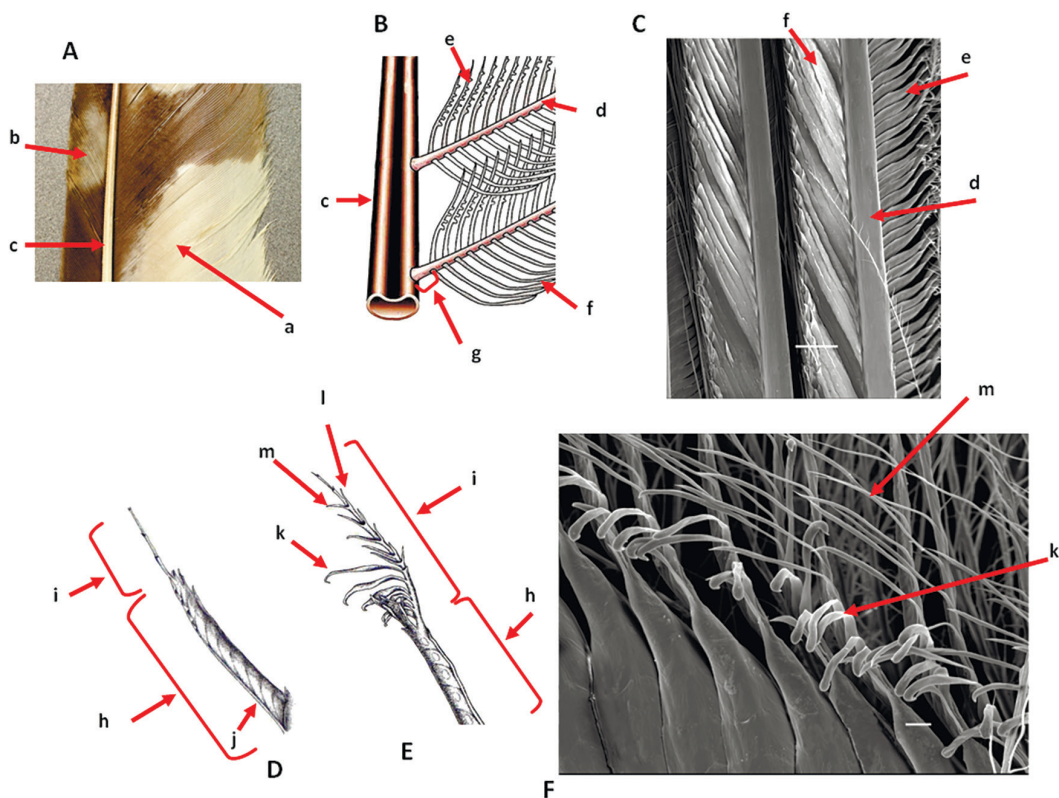


Fig. 1. Microstructure of the pennaceous barbs of a primary remex inner vane: *A* – a segment of a primary remex inner vane of a Long-Eared Owl *Asio otus*, a ventral surface; *B* – scheme of a segment of a contour feather inner vane (adapted from [33]); *C* – ventral surface of a primary remex inner vane of a Long-Eared Owl *Asio otus*. Pennaceous barbules of a remex inner vane: *D* – proximal barbule (adapted from [23]); *E* – distal barbule (adapted from [23]); *F* – distal barbules of a primary remex inner vane of a Long-Eared Owl *Asio otus* (*a* – inner vane; *b* – outer vane; *c* – rachis; *d* – ramus; *e* – distal barbules; *f* – proximal barbules; *g* – under vanules region of the pennaceous barb; *h* – base; *i* – pennulum; *j* – dorsal flange; *k* – hooklet; *l* – dorsal cilium; *m* – ventral cilium). Scanning electron micrographs (microscope JEOL-840A; scale: *C* – 100  $\mu\text{m}$ ; *F* – 10  $\mu\text{m}$ )

The barbs were thoroughly washed in distilled water, then dehydrated in ethanol series of increasing concentrations to acetone, dried in air and placed on the stage (a platform below the objective which supports the specimen being viewed), at the base of a MC-2 ZOOM binocular stereoscopic microscope intended for fine preparation.

The prepared barbs, including cross sections of barbs and longitudinal sections of barbs, were transferred to special aluminum sample stubs, where they were fixed with conductive glue designed for sample preparation. Preformed preparations were sprayed with gold with a thickness of 100–200 Å by the method of ion deposition under vacuum conditions on the Edwards S150A sputter coater (Great Britain), viewed and photographed using a JEOL-840A scanning electron microscope (SEM) (Japan), at accelerating voltage of 15 kV, in secondary electron imaging mode. The work was carried out in the Cabinet of electron microscopy of the A. N. Severtsov Institute of Ecology and Evolution of the Russian Academy of Sciences, Moscow.

Overall, 892 preparations of the pennaceous barbs of a primary remex of the studied species of Strigiformes were made, on the basis of which 2652 scanning electron micrographs were made and analyzed.

The analysis of the obtained scanning electron micrographs made it possible to investigate in detail the microstructural features of the primary remex in 13 species of Strigiformes and to compare the data obtained with the results of investigations conducted by us earlier.

The following microstructural characteristics were taken as the basis for the description of the fine structure of the primary remex: the configuration of the cross-section of the barb (Fig. 2); the structure of the medulla in a cross section of the barb and the structure of the medulla in the longitudinal section of the barb; the structure of the cuticula of the ramus: the relief of the cuticula, the configuration of the

cuticular cells; the microstructure of the vanules: a structure of proximal barbules, a structure of distal barbules, including the configuration of the free sections of the keratinized cuticular cells of the distal barbules, forming the dorsal surface of the vane.

The shape of cross-section of the ramus was determined based on the index of elongation (the ratio of the ramus cross section width to the ramus cross section length expressed in percentage) (Fig. 3, A). We used the method described in the work of Weger, Wagner [21] to evaluate the degree of the curvature of the ventral ridge (Fig. 3, B).

The effectiveness of the above characteristics of the fine structure of the primary remex using SEM for taxonomic identification of species has been proven by us in previous investigations [27, 28].

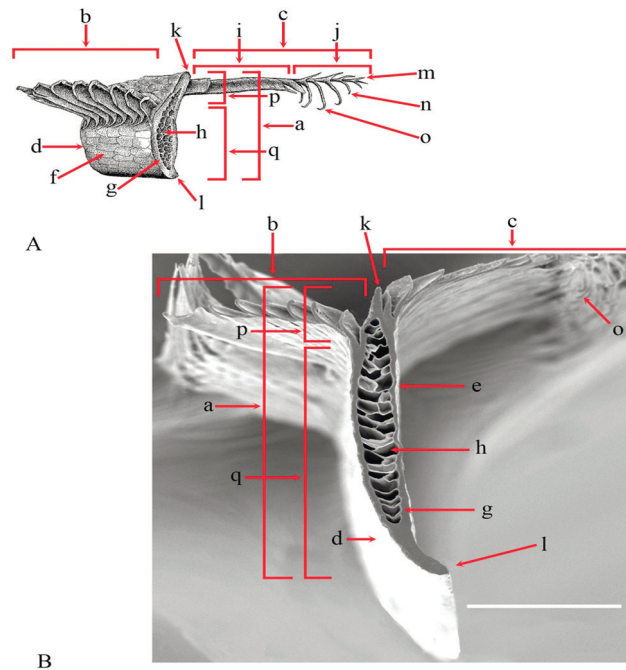


Fig. 2. Microstructure of the cross section of the ramus of a primary remex inner vane: A – segment of a pennaceous barb from a contour feather (adapted from [23]); B – cross section of the ramus of the Barn Owl *Tyto alba* primary remex inner vane pennaceous barb; the barb basal portion (a – ramus; b – proximal barbules; c – distal barbules; d – cuticula of the proximal lateral surface of the ventral part of the ramus; e – cuticula of the distal lateral surface of the ventral part of the ramus; f – cuticular cell; g – cortex; h – medulla; i – base; j – pennulum; k – dorsal ridge; l – ventral ridge; m – dorsal cilium; n – ventral cilium; o – hooklet; p – dorsal part of the ramus; q – ventral part of the ramus). Scanning electron micrograph (microscope JEOL-840A; scale: 100  $\mu$ m)

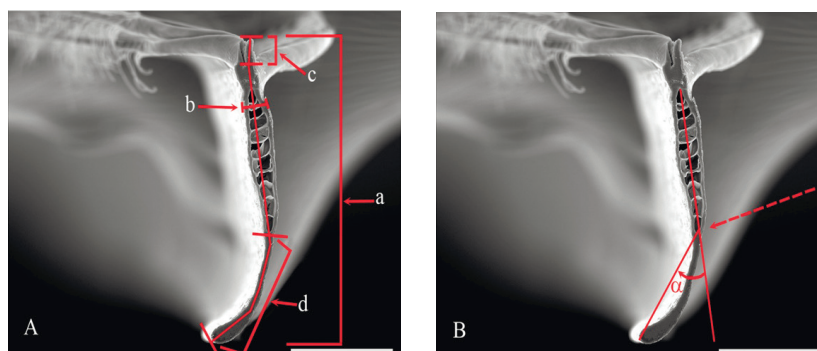


Fig. 3. Quantification of the ramus cross section configuration (cross section of the ramus of the Boreal Owl *Aegolius funereus* primary remex inner vane pennaceous barb; the pennaceous barb basal portion): A – four morphometric parameters of the cross section of the ramus: a – cross section length; b – cross section width; c – dorsal ridge length; d – ventral ridge length; B – tip displacement angle  $\alpha$  is the angle between the central longitudinal axis of the cross section of the ramus and the tip of the ventral ridge measured from the point of separation – base of the ventral ridge (it is indicated by the dotted arrow). Scanning electron micrographs (microscope JEOL-840A; scale: 100  $\mu$ m)

**Research results. Configuration of the cross section of the barb.** In the studied representatives of Strigiformes, the shape of the cross-section of the lower (basal) part of the pennaceous barb is species-specific due, first of all, to the variety of such structural details as the degree of flattening of the cross section from the lateral sides, the shape and ratio of the dorsal ridge and the ventral ridge, the nature of the curvature of the cross section.

The elongated, strongly flattened from the lateral sides willow-leaf shape of the cross section (limits of the elongation index are 4.8–6.3) was noted in *N. scandiaca*, *B. bubo*, *S. nebulosa*, *A. noctua*, and *A. otus*. Wherein, the greatest flatness (the elongation index is 4.8) was expressed in *B. bubo* and *A. noctua*. A less flattened lanceolate shape of the cross section (limits of the elongation index are 7.4–12.97) was noted in *T. alba*, *O. scops*, *O. sunia*, *S. aluco*, *S. uralensis*, *S. ulula*, *G. passerinum*, and *A. funereus*. Wherein, the most extended form of the cross section found in *T. alba*, *O. scops*, and *O. sunia* (elongation indices are 12.20; 10.59; 12.97 (see Table)).

In all the species of Strigiformes studied by us the dorsal ridge was insignificantly expressed; the ventral ridge, in contrast, was well developed and its length exceeded that of the dorsal ridge. The ventral ridge is the most elongated in *B. bubo*, *S. aluco*, *S. uralensis*, *G. passerinum*, *A. funereus*, *A. otus* and in *A. funereus* the ventral ridge has a thick club-shaped apex.

In addition, in all the species of Strigiformes studied by us, the ventral ridge is characterized by an arcuate-curved shape (limits of the curvature are 15°44'–44°39'). Wherein, the curvature of the ventral ridge most pronounced in *N. scandiaca*, *S. ulula*, and *A. noctua* (limits of the curvature are 35°00'–44°39' (see Table)).

The configuration of the cross section of the overlying portions of the barb (medial and distal portions) undergoes significant changes. The length is reduced, the width increases, due to which the cross section becomes more extended and rounded. So, a rounded ellipsoid cross section with fairly convex lateral surfaces is common in the distal part of the barb (limits of the elongation index are 28.13–52.36 (see Table)).

The ventral ridge in the distal part of the barb was severely shortened, dilated at the base, fairly curved (limits of the curvature are 26°49'–42°26') (*T. alba*, *O. scops*, *O. sunia*, *B. bubo*, *S. aluco*, *S. uralensis*, *S. ulula*, *G. passerinum*, *A. noctua*, *A. funereus*, *A. otus*). Less pronounced curvature of the ventral ridge in *S. nebulosa* (the curvature is 11°80') and *N. scandiaca* (the curvature is 14°47') (see Table).

Thus, in Strigiformes, the configuration of the cross section of the barb varies in direction from the base of the barb to its top: from the narrow, highly flattened willow-leaf shape in the basal part of the barb to the extended round shape in the upper distal part of the barb. One ridge passes in the middle of the dorsal part of the ramus and the other ridge passes in the middle of the ventral part of the ramus: the dorsal ridge and ventral ridge, respectively. The ridges are raised above the surface of the ramus, and the ridge on the ventral part of the ramus is significantly higher than the ridge on the dorsal part of the ramus, especially at the beginning of the basal part of the barb (proximal part), as a result, a strong bending of the ventral ridge is noted in the area of the attachment of the ramus to the rachis.

**Structure of the barb medulla.** Comparison of the architectonics of the medulla in the cross section of the barb and the longitudinal section of the barb allowed us to identify a number of features of the structure of the barb medulla, configuration features of the medullary air chambers and relief features of its walls (Fig. 4).

In all the studied species of Strigiformes, the medulla is absent under vanules of the barb (the place of the ramus attachment to the rachis (see Fig. 1, g)); cortex, completely filling the inner part of the barb, has an uniform structure. The medulla appears in the ramus area at the beginning of the basal part of the barb. In the overlying portions of the barb (medial and distal portions), the medulla begins to predominate in the internal structure of the ramus, while in the structure of the dorsal ridge and ventral ridge the medulla is still absent and the inside of both ridges is represented only with cortex. In general, the medulla of the barb is represented by a set of tightly packed medullary air chambers separated by thin walls.

At the cross section at the beginning of the basal part of the barb, the medulla has a single-row (*B. bubo* (the single-row medulla prevails), *S. uralensis*, *S. ulula* (Fig. 5, G), *A. noctua*, *N. scandiaca* (the single-row medulla prevails), *A. funereus*, *A. otus* (the single-row medulla prevails)), or one-two-row (*T. alba* (Fig. 5, A), *O. scops* (Fig. 5, C), *O. sunia*, *S. aluco*, *S. nebulosa*, *G. passerinum*) cellular, porous structure. In the subsequent medial part of the barb and the distal part of the barb, in almost all the studied species, the medulla is one-two-row and only *N. scandiaca* has a two-three-row medulla.

**Morphometric characteristics of the cross section of the ramus of the pennaceous barb of a primary remex inner vane of all Strigiformes species investigated**

Species	The cross section of the ramus of the pennaceous barb						The distal part of the pennaceous barb								
	The basal part of the pennaceous barb			The elongation index of the cross section, %			The cross section width, $\mu\text{m}$			The cross section length, $\mu\text{m}$			The elongation index of the cross section, %		
	<i>n</i>	The cross section width, $\mu\text{m}$	The cross section length, $\mu\text{m}$	The elongation index of the cross section, %	Angle $\alpha$ , degrees	<i>n</i>	The cross section width, $\mu\text{m}$	The cross section length, $\mu\text{m}$	The elongation index of the cross section, %	Angle $\alpha$ , degrees	<i>n</i>	The cross section width, $\mu\text{m}$	The cross section length, $\mu\text{m}$	The elongation index of the cross section, %	Angle $\alpha$ , degrees
<i>Tyto alba</i>	11	30.6867 ± 2.15370	253.6945 ± 1.657022	12.2033 ± 1.07598	29.7586 ± 0.412409	11	26.3933 ± 2.03431	69.7333 ± 1.069713	37.8800 ± 2.90814	38.3657 ± 0.450594					
<i>Otus scops</i>	12	25.4875 ± 0.92349	241.7079 ± 1.137632	10.5900 ± 0.92383	21.5600 ± 2.55850	12	26.0875 ± 2.38916	70.3908 ± 1.077201	37.2495 ± 1.49682	30.5590 ± 0.824247					
<i>Otus scuntia</i>	12	26.2075 ± 2.110282	202.4968 ± 1.684318	12.9650 ± 1.182554	15.4377 ± 0.682049	12	28.5775 ± 0.762818	54.6657 ± 1.078152	52.3584 ± 1.067547	27.6771 ± 0.787124					
<i>Nyctea scandiaca</i>	12	52.8500 ± 0.79662	842.1156 ± 1.713501	6.2785 ± 0.15897	35.0075 ± 2.85047	13	49.3800 ± 0.513452	150.4517 ± 1.626879	32.7178 ± 2.02393	14.4653 ± 0.441804					
<i>Bubo bubo</i>	15	128.348 ± 1.126087	2667.385 ± 1.560216	4.813 ± 0.3043	31.565 ± 0.9161	12	99.676 ± 0.738078	314.453 ± 1.614307	31.746 ± 2.5284	26.491 ± 0.9688					
<i>Strux aluco</i>	12	36.4648 ± 1.597484	429.7054 ± 1.627101	8.5364 ± 1.75156	28.6674 ± 0.625274	10	35.8100 ± 2.06475	114.9357 ± 1.835587	31.3550 ± 0.96874	27.4697 ± 1.050445					
<i>Strux uralensis</i>	10	35.1200 ± 1.38593	473.3533 ± 1.630208	7.4240 ± 0.17819	31.8350 ± 1.80312	10	40.4073 ± 1.058509	143.3437 ± 1.717346	28.1300 ± 0.39598	42.2614 ± 0.575136					
<i>Strix nebulosa</i>	13	39.4429 ± 1.021253	672.5941 ± 1.657810	5.8852 ± 0.74162	30.7514 ± 1.132143	14	33.1800 ± 2.93957	97.7272 ± 2.421718	34.2083 ± 2.44624	11.7967 ± 0.97977					
<i>Surnia ulula</i>	13	31.6560 ± 0.903178	345.4024 ± 1.117767	9.1710 ± 0.415112	38.2060 ± 1.290994	12	31.6408 ± 1.094696	85.6493 ± 1.205178	37.1640 ± 1.670812	40.6950 ± 0.816497					
<i>Glauclidium passerinum</i>	12	16.5125 ± 0.745447	185.3748 ± 1.034376	8.9247 ± 0.517974	25.0650 ± 1.564236	10	18.3700 ± 1.032376	60.3650 ± 2.877925	30.5379 ± 1.131569	39.3437 ± 1.146597					
<i>Athene noctua</i>	11	21.4933 ± 0.55474	445.2539 ± 1.648782	4.8333 ± 0.16653	44.3943 ± 0.436992	11	24.4200 ± 1.02196	73.4884 ± 1.574784	33.6700 ± 1.099151	28.9600 ± 1.08972					
<i>Aegolius funereus</i>	10	22.5950 ± 0.685894	245.0450 ± 0.926310	9.2200 ± 0.240416	28.5900 ± 1.711198	14	26.0850 ± 1.341712	53.8650 ± 2.716606	48.59557 ± 1.078750	28.38571 ± 1.162252					
<i>Asio otus</i>	11	33.8633 ± 0.65623	549.6296 ± 1.683541	6.1600 ± 0.18520	32.3657 ± 0.70590	10	36.2400 ± 1.49907	83.2400 ± 2.12132	43.5300 ± 0.69296	39.4529 ± 0.59056					

Note. *n* – number of measured cross sections, angle  $\alpha$  – the angle between the central longitudinal axis of the cross section of the ramus and the tip of the ventral ridge measured from the point of separation – the base of the ventral ridge.

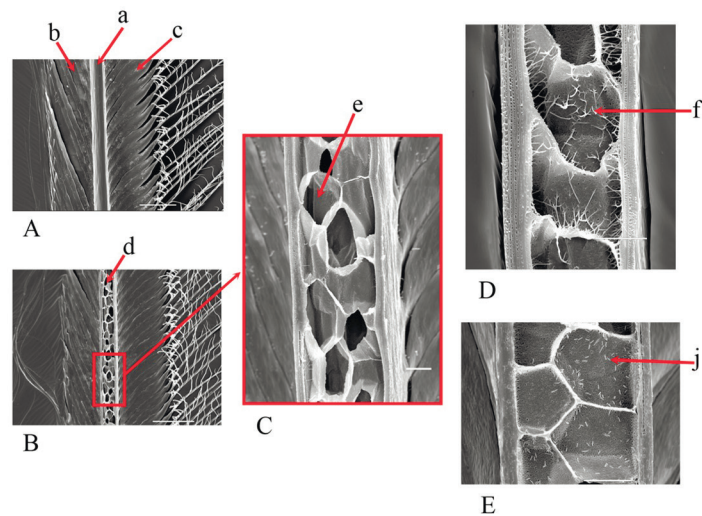


Fig. 4. Medulla in the longitudinal section of the ramus of the primary remex inner vane pennaceous barb: *A* – ventral surface of a Barn Owl *Tyto alba* pennaceous barb; the medulla in the longitudinal section of the ramus of a pennaceous barb: *B*, *C* – in the Barn Owl *Tyto alba*, *D* – in the Eurasian Scops Owl *Otus scops*, *E* – in the Boreal Owl *Aegolius funereus* (*a* – ramus; *b* – proximal barbules; *c* – distal barbules; *d* – the longitudinal section of the ramus; *i* – medullary chamber; *f* – keratin filaments; *j* – pigment granules). Scanning electron micrographs (microscope JEOL-840A; scale: *A*, *B* – 100  $\mu\text{m}$ ; *C*–*E* – 10  $\mu\text{m}$ )

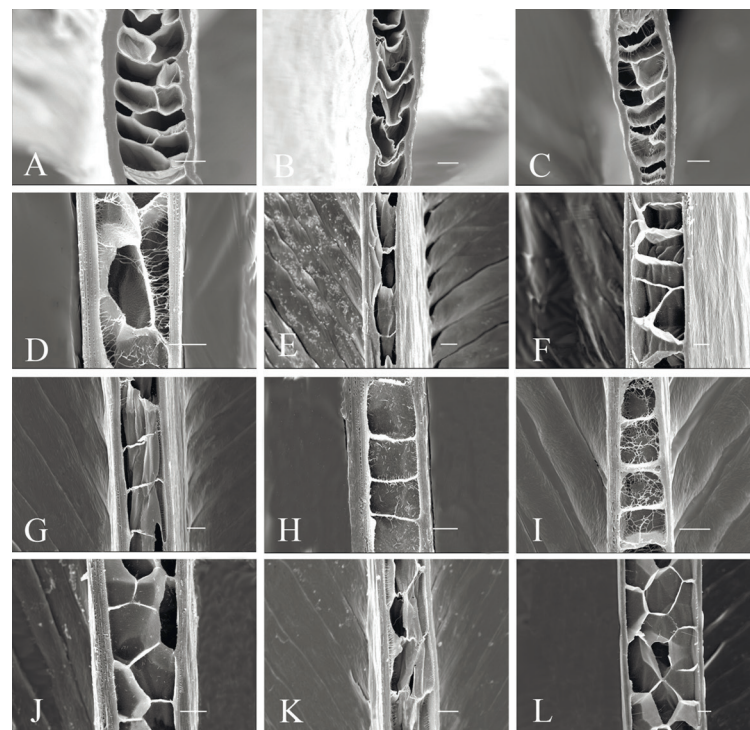


Fig. 5. Medulla of the ramus of the Strigiformes primary remex: the cross section of the ramus (*A* – *Tyto alba*; *B* – *Surnia ulula*; *C* – *Otus scops*) and the longitudinal section of the ramus (*D* – *Otus scops*; *E* – *Tyto alba*; *F* – *Strix nebulosa*; *G* – *Surnia ulula*; *H* – *Surnia ulula*; *I* – *Surnia ulula*; *J* – *Strix uralensis*; *K* – *Glaucidium passerinum*; *L* – *Nyctea scandiaca*). Scanning electron micrographs (microscope JEOL-840A; scale: 10  $\mu\text{m}$ )

On the longitudinal section at the beginning of the basal part of the barb, the medulla in the most of the studied species is a mixed one-two-row, and in only *T. alba* (Fig. 5, *E*), *B. bubo*, *A. noctua* and the medulla is a single-row. In the subsequent parts of the barb, in most species, the one-two-row structure of the medulla is found more often than two-row (*A. noctua*) or two-three-row (*T. alba*, *N. scandiaca* (Fig. 5, *L*). In the upper apical part of the barb, the medulla in most of the studied species is single-row.

Thus, in the central part of the ramus, there is the medulla formed by chambers arranged in regular rows, the number of which varies in different parts of the barb.

The configuration of the medullary air chambers is quite diverse. On the cross section in the basal part of the barb we found the flattened form of the transverse chambers (*N. scandiaca*, *B. bubo*, *S. uralensis*, *A. funereus*), and the flatness of the chambers may vary considerably. V-shaped curved chambers are less common (*S. ulula* (Fig. 5, B), *A. noctua*, *A. otus*). In addition, we found the medulla of the mixed type, formed by the alternation of rounded and flattened medullary air chambers (*T. alba* (Fig. 5, A), *O. scops* (Fig. 5, C), *O. sunia*, *S. aluco*, *S. nebulosa*, *G. passerinum*).

In the structure of the medulla on the cross section in the subsequent parts of the barb in the overwhelming majority of species there is an alternation of rounded and flattened chambers (*T. alba*, *O. sunia*, *N. scandiaca*, *B. bubo*, *S. uralensis*, *S. ulula*, *A. noctua*); the predominance of flattened chambers is in *S. nebulosa* and *A. otus*, rounded – in *O. scops* and *A. funereus*. Thus, only in *O. sunia*, *S. aluco* and *G. passerinum* the uniform configuration of chambers on the cross section was noted in the structure of the medulla throughout the barb. The longitudinal section also revealed a difference in the configurations of the medullary chambers in different parts of the barb.

The relief of the medullary chambers walls is not equally pronounced in different parts of the barb. Thus, in the cross section in the basal part of the barb, the large-wavy relief of the chambers walls (Fig. 5, B, C) is noted in all the studied species, with the exception of *T. alba* (Fig. 5, A), which has a smooth, slightly wavy relief of the chambers walls. In the subsequent parts of the barb, the large-wavy surface of the chambers walls is noted in all the studied species. In the longitudinal section of the barb, the vast majority of the studied species have alternating chambers with large-plicated (Fig. 5, E, G, K), large-wavy (Fig. 5, D, F, L), less often smooth walls (Fig. 5, H, I): *T. alba* (Fig. 5, E), *O. scops* (Fig. 5, D), *O. sunia*, *N. scandiaca* (Fig. 5, L), *B. bubo*, *S. aluco*, *S. nebulosa* (Fig. 5, F), *S. ulula* (Fig. 5, G, H, I) (deep longitudinal plicate of the chambers walls in the beginning of the basal part of the barb (Fig. 5, G)), *G. passerinum* (Fig. 5, K), *A. noctua*, *A. funereus*, and *A. otus*. The smooth or slightly wavy relief of the medullary chambers walls distinguishes *S. uralensis* (Fig. 5, J).

In addition to the features described above, the presence or absence of keratin filaments forming the medullary chambers framework and pigment granules on the chamber walls can be a significant addition to the complex characteristic of the barb medulla.

The structure of the inner filamentous framework of the medullary chambers looks differently on the cross section and on the longitudinal sections in different parts of the barb. On the cross section in the basal part of the barb the absence of the filamentous framework was noted in *A. funereus*; occasionally, groups of short and long threads were found in the medullary chambers framework in *T. alba* (Fig. 5, A), *O. sunia*, *N. scandiaca*, *B. bubo*, *S. aluco*, *S. uralensis*, *S. nebulosa*, *S. ulula* (Fig. 5, B), *G. passerinum*, *A. noctua*, and *A. otus*; keratin filaments occurring in all the medullary chambers, but unevenly (in some medullary chambers the filaments are rare, in others – quite numerous), noted in *O. scops* (Fig. 5, C). On the cross section in the subsequent parts of the barb an uneven distribution of the filaments with the formation of individual thick accumulations predominates (*T. alba*, *O. scops*, *O. sunia*, *S. aluco*, *S. uralensis*, *S. nebulosa*, *S. ulula*, *G. passerinum*, *A. noctua*); occasionally occurring filaments groups were still noted in *N. scandiaca*, *B. bubo*, *A. otus*; and *A. funereus* had practically no filaments, there were small groups of small, very short filaments only in some medullary chambers. In the longitudinal section of the barb, few filaments were found in the medullary chambers framework in *T. alba* (Fig. 3, C; Fig. 5, E), *N. scandiaca* (Fig. 5, L), *S. aluco*, *S. uralensis* (Fig. 5, J), *S. nebulosa* (Fig. 5, F), *G. passerinum* (Fig. 5, K), *A. noctua*, *A. funereus*, and *A. otus*; abundance of filaments in the framework of the medullary chambers was found in *O. scops* (Fig. 4, D) and *O. sunia*. The uneven distribution of the filaments of the medullary chambers framework was noted in *B. bubo* and *S. ulula* (Fig. 5, G, H, I): the filaments, which are weakly expressed in the lower parts of the barb (the occurrence of filaments is 22.22–40.74 % in *B. bubo*; 16.67–50 % in *S. ulula*), form thick plexuses in the upper distal part of the barb (Fig. 5, I) (the occurrence of filaments is 70–85 % in *B. bubo*; 88.89 % in *S. ulula*). The occurrence of filaments in medullary chambers in a certain part of the longitudinal section of the barb was evaluated as a percentage of accounting portions with the presence of filaments from the total number of accounting portions in this part of the longitudinal section of the barb.

Pigment granules on the walls of the medullary chambers were not found in *T. alba* (Fig. 4, C; Fig. 5, A, E), *N. scandiaca* (Fig. 5, L), and *S. nebulosa* (Fig. 5, F). In the other species studied, the pigment granules were absent only in the basal part of the barb in the cross section. At the same time, in the overwhelming majority of species disseminations of pigment granules were relatively evenly distributed in the medullary air chambers throughout the barb (Fig. 4, E; Fig. 5, J). In *S. ulula*, pigment granules are unevenly distributed, sometimes forming quite numerous accumulations in separate medullary chambers in the longitudinal section of the barb (Fig. 5, H).

**Structure of cuticula of ramus.** The structure of the cuticula of the ramus in all the species of the Strigiformes studied by us undergoes noticeable changes in the direction from the base of the barb to its top. Besides, differences were noted in the configuration of the cuticular cells of each of the two lateral surfaces (distal and proximal) of the ramus, which is consistent with the results of our previous investigations [25, 26, 29–31].

Due to the above, for comparative analysis, we selected a specific area of the cuticula of the ramus – the distal lateral surface of the ventral part of the ramus in the basal part of the barb.

In all the species of Strigiformes studied by us, cuticular cells were oblong, longitudinally oriented, tightly closed. In the majority of the species studied (*O. scops*, *O. sunia*, *N. scandiaca* (Fig. 6, B), *B. bubo* (Fig. 6, A), *S. aluco*, *S. nebulosa*, *A. otus* (Fig. 6, E)), the edges of the cuticular cells were thickened and well expressed (limits of the width are 1.0–3.73  $\mu\text{m}$ ). Especially well expressed edges of cells were found in *N. scandiaca* (the width is  $3.73 \pm 0.66 \mu\text{m}$ ). Slightly thickened edges of cuticular cells (limits of the width are 0.69–0.75  $\mu\text{m}$ ) were found in *S. ulula* (Fig. 6, F), *A. noctua*, and *A. funereus*. Cuticular cells with not thickened (limits of the width are 0.23–0.40  $\mu\text{m}$ ), weakly pronounced edges were noted in *T. alba* (Fig. 6, D), *S. uralensis*, and *G. passerinum* (Fig. 6, C).

The relief of the surface of the cuticular cells in all studied species was smoothed, fibrous, represented by tightly fitting and intertwining fibers, while in *G. passerinum* (Fig. 6, C) and *T. alba* (Fig. 6, D) we revealed distinct separated plexuses of large fibers over the main dense fibrous structure of the cuticular surface. In all studied species slightly convex ring-shaped structures were noted on the surface of the cuticular cells, especially expressed in *N. scandiaca* (numerous, found in almost every cell) (Fig. 6, B), *B. bubo* (Fig. 6, A) and *A. otus* (Fig. 6, E), less clearly – in *G. passerinum* and *A. noctua*, weakly

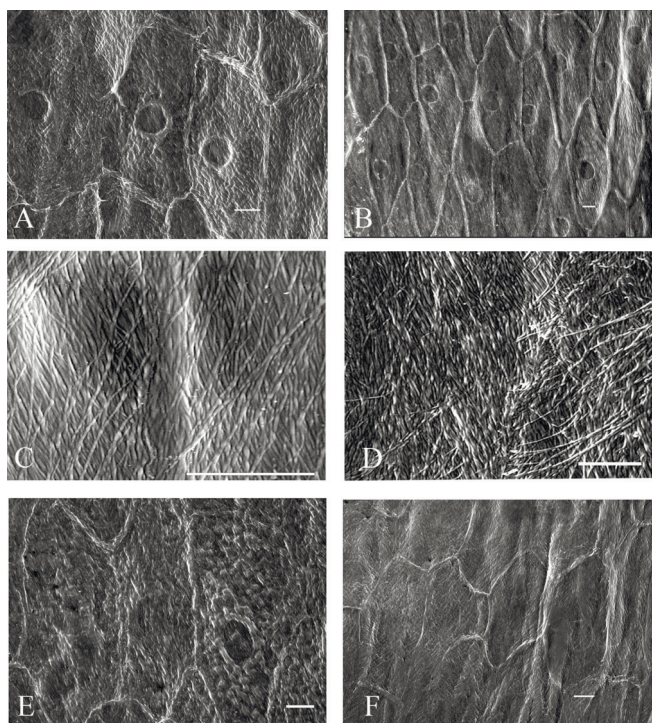


Fig. 6. Relief of the cuticular cells surface of the ramus of the Strigiformes primary remex: A – in *Bubo bubo*; B – in *Nyctea scandiaca*; C – in *Glaucidium passerinum*; D – in *Tyto alba*; E – in *Asio otus*; F – in *Surnia ulula*. Scanning electron micrographs (microscope JEOL-840A; scale: 10  $\mu\text{m}$ )

expressed in *T. alba* (rarely encountered), *O. scops*, *O. sunia*, *S. aluco* (rarely encountered), *S. uralensis*, *S. nebulosa*, *S. ulula* (rarely encountered) (Fig. 6, *F*), and *A. funereus* (rarely encountered).

Thus, a comparative analysis of a strictly defined area of the cuticula, namely the distal lateral surface of the ventral part of ramus in the basal portion of barb, revealed a number of structural features of the cuticula in Strigiformes: elongated and longitudinally oriented cells with a smoothed fibrous relief of the surface, a presence of the thickened edges of cells in the majority of studied species, and specific slightly convex ring-shaped structures, the manifestation degree of which varies in different species of Strigiformes studied by us.

**Microstructure of vanules.** Vanules are a set of proximal barbules and distal barbules, branch out the ramus to both sides and uniformly distributed along the entire length of the ramus – not far from the point of attachment of the barb to the rachis, to its top (Fig. 1, *B*) [23, 29–31].

In Strigiformes, proximal barbules have in their structure elements typical for representatives of other groups of birds studied by us earlier: an extended base with a characteristic curved dorsal edge (dorsal flange) and a very elongated needle-like pennulum (Fig. 1, *D*). The proximal barbules tightly adjoin with each other in the basal part of the barb and in the medial part of the barb, and friably located in the distal part of the barb.

In the structure of the distal barbules in the Strigiformes, typical traits are the extended base and the subsequent pennulum – a thin elongated part of the distal barbule with a complex of free parts of keratinized cuticular cells: hooklets (Fig. 1, *k*) at the basal part of the pennulum on its lower – ventral – side, as well as thin outgrowths (dorsal cilia and ventral cilia) throughout the pennulum, including its apical part (Fig. 1, *E*).

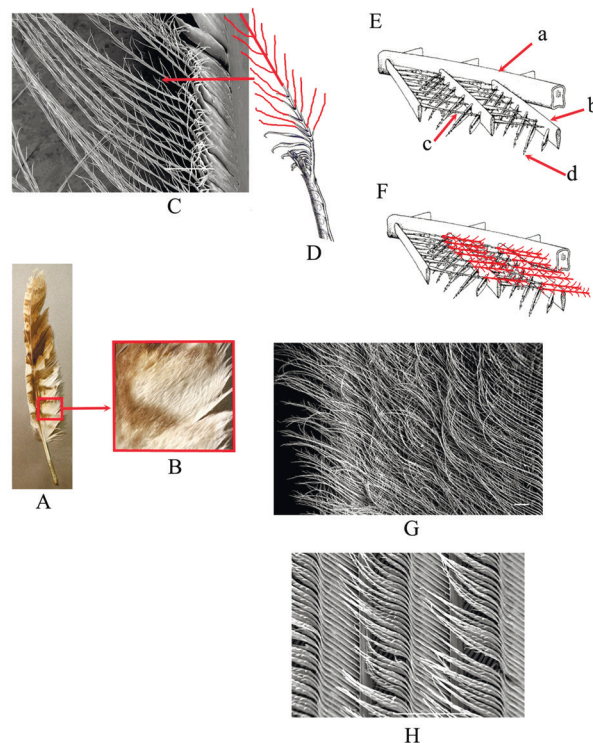


Fig. 7. Specific features in the microstructure of the distal barbules of Owls (Strigiformes) which make for the velvet-like dorsal surface of the inner vane of a primary remex: *A* – the whole primary remex of a Tawny Owl *Strix aluco*, a dorsal surface; *B* – segment of the velvet-like dorsal surface of the Tawny Owl *Strix aluco* primary remex inner vane; *C* – distal barbules with numerous hairlike cilia of a Little Owl *Athene noctua* primary remex inner vane; *D* – distal barbules; the elongated pennulum with hairlike cilia is shown in the red (adapted from [23]); *E* – scheme of a segment of a contour feather inner vane; the pennulums of distal barbules are not elongated: *a* – rachis; *b* – ramus; *c* – distal barbules; *d* – proximal barbules (adapted from [38]); *F* – scheme of a segment of the Owls (Strigiformes) contour feather inner vane; the aggregate of the elongated pennulums forms the thick velvet-like dorsal surface of the inner vane; it is represented by red (adapted from [38]). Microstructure of the primary remex inner vane dorsal surface: *G* – thick velvet-like dorsal surface of the Owls (Strigiformes) inner vane (Tawny Owl *Strix aluco*); *H* – non-velvety dorsal surface of the inner vane (Short-Toed Snake Eagle *Circaetus gallicus*). Scanning electron micrographs (microscope JEOL-840A; scale: *C*, *G* – 100  $\mu\text{m}$ ; *H* – 1  $\mu\text{m}$

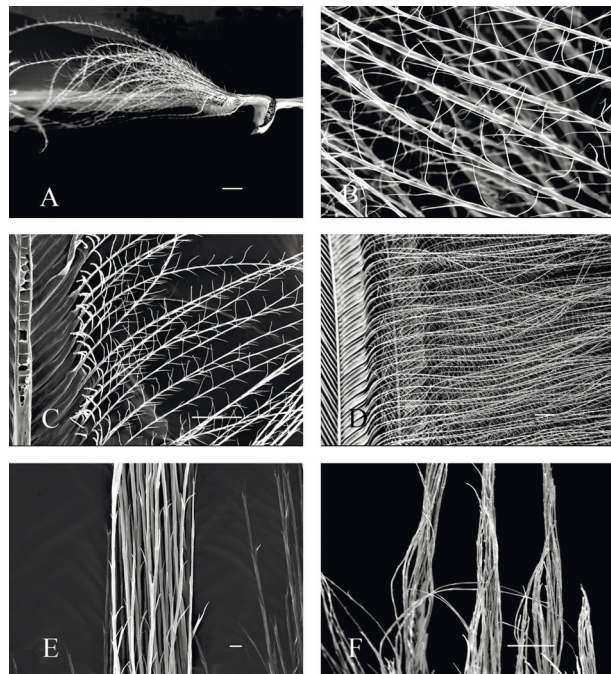


Fig. 8. Microstructure of the pennaceous barb vanules of the Strigiformes primary remex inner vane: *A* – segment of a pennaceous barb with distal barbules (*Strix nebulosa*); distal barbules with numerous cilia (*B* – in *Tyto alba*; *C* – in *Surnia ulula*); *D* – the dense fleecy structure of the primary remex vane dorsal surface (*Strux aluco*); *E* – barb apical section elongate proximal barbules and the distal barbules closed together (*Surnia ulula*); *F* – cleft edge of the primary remex inner vane (*Glaucidium passerinum*). Scanning electron micrographs (microscope JEOL-840A, scale: *B, E* – 10 μm; *A, C–D, F* – 100 μm)

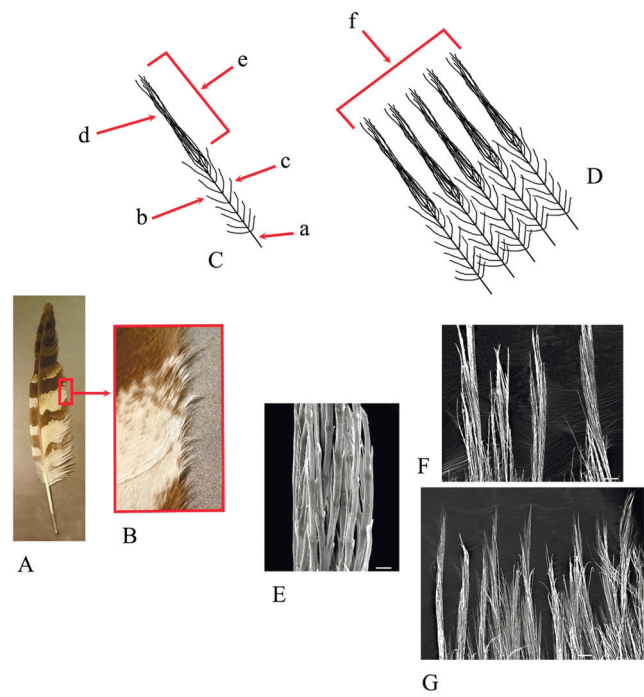


Fig. 9. Specific features in the microstructure of the barbs of Owls (Strigiformes) which make for the cleft edge of the inner vane of a primary remex: *A* – whole primary remex of a Great Grey Owl *Strix nebulosa*, a dorsal surface; *B* – cleft edge of the Great Grey Owl *Strix nebulosa* primary remex inner vane, a dorsal surface; *C* – “bunch” in the distal part of the barb (*a* – ramus; *b* – distal barbules; *c* – proximal barbules; *d* – elongated tightly closed barbules in the distal part of the barb; *e* – “bunch”); *D* – row of “bunches” forms the cleft edge of the inner vane (*f* – cleft edge of the inner vane). Microstructure of the Owls (Strigiformes) primary remex inner vane dorsal surface: *E* – elongated tightly closed barbules in the distal part of the barb (Eurasian Pygmy Owl *Glaucidium passerinum*); cleft edge of the inner vane: *F* – in Great Grey Owl *Strix nebulosa*; *G* – in Northern Hawk-Owl *Surnia ulula*. Scanning electron micrographs (microscope JEOL-840A; scale: *E* – 10 μm; *F, G* – 100 μm)

A specific feature in the structure of the distal barbules of the Strigiformes is a very elongated pennulum with numerous well-developed hairlike cilia (Fig. 7; Fig. 8, A–C), which make for, as a whole, the thick velvet-like dorsal surface of the vane of a primary remex (Fig. 7; Fig. 8, D).

Due to the tight adjoining highly elongated barbules to each other and to the apical portion of the ramus, the distinctive “bunch”, also known as a fringe [17, 19, 22], is formed (Fig. 8, E; Fig. 9, C, E). A row of these “bunches” forms the cleft edge (Fig. 8, F; Fig. 9, f, F, G), also known as fringes [17, 19, 22], of the inner vane, well expressed in all species of Strigiformes studied by us. At the same time, the degree of the cleavage of the edge of the inner vane in *N. scandiaca* is less expressed than the other species studied by us, that which is consistent with the results of our previous studies [25, 26, 29, 30].

**Discussion.** The results obtained by us in the course of this comparative investigation of the microstructure of the Strigiformes primary remex are completely consistent with the results of our earlier studies of the microstructural features of the Strigiformes contour feather [25, 26, 29–31]. A number of microstructural characteristics of feathers detected in Strigiformes are also noted to varying degrees in other groups of birds examined by us [28, 36, 37]: an elongated, very flattened shape of the cross section of the basal part of the pennaceous barbs and a significant change in the configuration of the cross section of the overlying areas of barb; the barb medulla topography and structural diversity of the medullary chambers, including the presence of keratin filaments and pigment granules; a diversity in the structure of cuticular cells (shape, thickened edges, surface relief, the presence of slightly convex ring-shaped structures) and pronounced differences in the ornament of the cuticula relief in different parts of the ramus, including differences in the configuration of the cuticular cells of each of the two lateral surfaces of the ramus (distal and proximal), especially in the ventral part of the ramus.

It should be emphasized that, in Strigiformes, as well as in representatives of other bird groups studied by us, the identified microstructural characteristics of the feather significantly differ not only in different parts of one and the same barb, but also in barbs taken from different parts of the vanes [36].

A number of characteristics, identified as a result of a comparative investigation of the microstructure of the vanules of the primary remex pennaceous barb of Strigiformes, are unique and distinguish all Strigiformes from representatives of other bird groups.

First of all, this is the specificity of the distal barbules: a very elongated pennulum with numerous well-developed hairlike cilia located on it. The aggregate of the pennulums tightly contiguous to the proximal barbules and not intertwining with each other forms, as a whole, the thick velvet-like dorsal surface of the vane.

In the literature, there are little mentions of the velvet-like dorsal surface of the vane of a primary remex of Strigiformes, and there is no description of the microstructural features of the distal barbules that cause this velvet-like structure. Usually, the characteristic of a feather structure in Strigiformes is limited to the phrases that “the plumage is soft, friable, fluffy; remiges are relatively soft, velvety” [39], “remiges of Owls are relatively soft” [2], “fluffy surface of the plumage” [40], “softness of the contour feathers” [4]. Besides that, it is noted that the Snowy Owl and the Northern Hawk-Owl, “compelled to hunt in conditions of the white nights or the polar day”, as well as Little Owls and Pygmy-Owls, have “tough a plumage, as in raptors” [2].

The presence of the velvet-like dorsal surface of the vane was recorded only in the Barn Owl [17–22]. According to our data, the thick velvet-like dorsal surface of the vane is characteristic of all studied species of Strigiformes, including a Snowy Owl, a Northern Hawk-Owl, a Boreal Owl, a Little Owl, and a Eurasian Pygmy Owl and significantly differs from the smoothed dorsal surface of the vane in representatives of raptors (Fig. 7, H).

The presence of the cleft edge of the primary remex inner vane of Strigiformes is a well-known fact. The adaptive nature of the cleft edge of the inner vane of Strigiformes, associated with their noiseless flight in the night-time, is proved [17–22]. Nevertheless, the microstructure of the cleft edge of the inner vane – at the SEM level – has not yet been examined in detail.

Our investigation fills up this gap. Identified features in the structure of the cleft edge of the primary remex inner vane of the studied species of Strigiformes, introduce essential corrections to the question about the formation of the fringes at the edge of the inner vane in Strigiformes.

Previously, it was erroneously noted that the fringes form where the tips of the barbs are separated due to a loss of hooklets on the hook radiates, which leads to unconnected barb ends [17, 19, 21, 22].

Our electron microscopic investigation of the microstructure of the fringed edge of the primary remex inner vane of Strigiformes, carried out using a scanning electron microscope, made it possible to investigate this question in detail and identified a number of the unique features in the microstructure of the vanules which make for the fringes at the edge of the inner vane in Strigiformes (the elongated barbules are tightly closed with each other and with the apical portion of the ramus and form the distinctive “bunch” (a fringe); a row of these “bunches” (fringes), in turn, forms the cleft edge (a fringed edge) of the inner vane) (Fig. 9).

In our opinion, the identified elements of the microstructure of the vanules of the primary remex pennaceous barb in Strigiformes – the most important functional element of the wing of birds – have an adaptive character associated with the features of specialization to the specific style of hunting in the night-time, in particular – with a noiseless flight. It is noteworthy that the degree of the cleavage of the edge of the vane in *N. scandiaca* is less pronounced than in other species of Strigiformes studied by us. Note that *N. scandiaca* is a unique predator capable, unlike most other species of Strigiformes, to hunt equally well at a night-time as well as at a day-time.

**Conclusion.** Thus, as a result of our comparative electron microscopic investigation of the microstructure of the primary remex of Strigiformes, a number of microstructural characteristics have been identified. These microstructural characteristics of the barb can be used in further studies on the comparative morphology of bird feathers. In this aspect, the configuration of the cross section, the structure of the medulla, the shape and relief of the surface of the cuticular cells are important.

The analysis showed that in Strigiformes, as well as in representatives of other bird groups studied by us, the identified microstructural characteristics of the feather significantly differ not only in different parts of one and the same barb, but also in barbs taken from different parts of the vanes.

A number of the characteristics revealed as a result of the carried out comparative research of the microstructure of the vanules of the primary remex pennaceous barb of Strigiformes are unique, distinguishing all Strigiformes from representatives of other groups of birds. First of all, these are the structural features of the distal barbules and the structure of the apical portion of the barb with the elongated proximal barbules and the distal barbules tightly contiguous to the ramus and closed with each other. Mentioned characteristics make for the thick velvet-like dorsal surface of the vane and the presence of a complex of peculiar “bunches” (fringes) forming the cleft edge (a fringed edge) of the inner vane – exceptionally specific feather features in Strigiformes which are not found more at any representatives of other bird groups investigated by us. The features of the microstructure of the vanules that we identified are the first detailed information on the morphology – at the SEM level – of the specific elements of the feather in Strigiformes, which are considered in modern literature [16–22] as structures that make for a noiseless flight. Apparently, the noted features of the microstructure of the vanules can be considered as eco-morphological adaptations keeping the basic structure of the feather and directed to the formation of specific aerodynamic effects of the wing of Strigiformes.

The results obtained provide witness that the identified basic specific characteristics of the primary remex microstructure of Strigiformes can be used to study the direction and dynamics of complex radiation of morphological and adaptational changes of the feather microstructure in the birds phylogenesis.

## References

1. Il'ichev V. D., Bogoslovskaya L. S., Barsova L. I. Central sections of the auditory system of birds. Morpho-ecological analysis of the structure of the auditory nuclei of the medulla oblongata. *Zoologicheskii zhurnal* [Zoological journal], 1974, vol. 53, no. 9, pp. 1352–1362 (in Russian).
2. Pukinskii Yu. B. *The life of Owls*. Leningrad, Leningrad University Publishing House, 1977. 240 p. (in Russian).
3. Mikkola H. *Owls of Europe*. Carlton, T&D Poyse, 1983. 397 p.
4. Gavrilov E. I., Ivanchev V. P., Kotov A. A., Koshelev A. I., Nazarov Yu. N., Nechaev V. A., Numerov A. D., Priklonskii S. G., Pukinskii Yu. B., Rustamov A. K. *Birds of Russia and adjacent regions: Pterocletiformes, Columbiformes, Cuculiformes, Strigiformes*. Moscow, Nauka Publ., 1993. 400 p. (in Russian).
5. Duncan J. R. *Owls of the world: their lives, behavior and survival*. New York, Firefly Books, 2003. 319 p.
6. Duncan J. R. *Owls of the World*. New Holland Publishers. New South Wales, Australia, Chatswood, 2016. 240 p.

7. But'ev V. T., Zubkov N. I., Ivanchev V. P., Koblik E. A., Kovshar' A. F., Kotyukov Yu. V. [et al.]. *Birds of Russia and adjacent regions: Strigiformes, Caprimulgiformes, Apodiformes, Coraciiformes, Upupiformes, Piciformes*. Moscow, KMK Scientific Publishing Partnership, 2005. 487 p. (in Russian).
8. Volkov S. V., Sharikov A. V., Morozov V. V. (eds). *Owls of the Northern Eurasia*. Moscow, 2005. 472 p. (in Russian).
9. Volkov S. V., Sharikov A. V., Morozov V. V. (eds). *Owls of the Northern Eurasia: Ecology, spatial and habitat distribution*. Moscow, 2009. 304 p. (in Russian).
10. Wink M., El-Sayed A.-A., Sauer-Gürth H., Gonzalez J. Molecular phylogeny of owls (Strigiformes) inferred from DNA sequences of the mitochondrial cytochrome b and the nuclear RAG-1 gene. *Ardea*, 2009, vol. 97, no. 4, pp. 581–591. <https://doi.org/10.5253/078.097.0425>
11. König C., Weick F., Becking J. *Owls of the world. 2nd ed.* London, Christopher Helm, 2011. 528 p.
12. Romulo C. L. *Geodatabase of global owl species and owl biodiversity analysis*. Falls Church, Virginia, Virginia Polytechnic Institute and State University, Master of Natural Resources Capstone Paper, 2012. 53 p.
13. Koch U. R., Wagner H. Morphometry of auricular feathers of Barn Owls (*Tyto alba*). *European Journal of Morphology*, 2002, vol. 40, no. 1, pp. 15–21. <https://doi.org/10.1076/ejom.40.1.15.13957>
14. Lin W.-L., Lin S.-M., Tseng H.-Y. Colour morphs in the Collared Pygmy Owl *Glaucidium brodiei* are age-related, not a polymorphism. *Ardea*, 2014, vol. 102, no. 1, pp. 95–99. <https://doi.org/10.5253/078.102.0115>
15. Charter M., Leshem Y., Izhaki I., Roulin A. Pheomelanin-based colouration is correlated with indices of flying strategies in the Barn Owl. *Journal of Ornithology*, 2015, vol. 156, no. 1, pp. 309–312. <https://doi.org/10.1007/s10336-014-1129-6>
16. Sarradj E., Fritzsche C., Geyer T. Silent owl flight: bird flyover noise measurements. *AIAA Journal*, 2011, vol. 49, no. 4, pp. 769–779. <https://doi.org/10.2514/1.j050703>
17. Bachmann T., Wagner H., Tropea C. Inner vane fringes of barn owl feathers reconsidered: morphometric data and functional aspects. *Journal of Anatomy*, 2012, vol. 221, no. 1, pp. 1–8. <https://doi.org/10.1111/j.1469-7580.2012.01504.x>
18. Klän S., Burgmann S., Bachmann T., Klaas M., Wagner H., Schröder W. Surface structure and dimensional effects on the aerodynamics of an owl-based wing model. *European Journal of Mechanics – B/Fluids*, 2012, vol. 33, pp. 58–73. <https://doi.org/10.1016/j.euromechflu.2011.12.006>
19. Winzen A., Roidl B., Klän S., Klaas M., Schröder W. Particle-image velocimetry and force measurements of leading-edge serrations on owl-based wing models. *Journal of Bionic Engineering*, 2014, vol. 11, no. 3, pp. 423–438. [https://doi.org/10.1016/s1672-6529\(14\)60055-x](https://doi.org/10.1016/s1672-6529(14)60055-x)
20. Sagar P., Teotia P., Sahlot A. D., Thakur H. C. An analysis of silent flight of owl. *Materials Today: Proceedings*, 2017, vol. 4, no. 8, pp. 8571–8575. <https://doi.org/10.1016/j.matpr.2017.07.204>
21. Weger M., Wagner H. Morphological variations of leading-edge serrations in owls (strigiformes). *PLoS ONE*, 2016, vol. 11, no. 3, p. e0149236. <https://doi.org/10.1371/journal.pone.0149236>
22. Weger M., Wagner H. Distribution of the characteristics of barbs and barbules on barn owl wing feathers. *Journal of Anatomy*, 2017, vol. 230, no. 5, pp. 734–742. <https://doi.org/10.1111/joa.12595>
23. Lucas A. M., Stettenheim P. R. *Avian anatomy. Integument. Agriculture handbook 362*. Washington, D. C., U. S. Government Printing Office, 1972. 340 p.
24. Stettenheim P. R. Structural adaptations in feathers. *Proceedings of the 16th International Ornithological Congress*. Canberra, Australia, 1976, pp. 385–401.
25. Fadeeva E. O. Adaptability particularities of the snowy owl's (*Nyctea scandiaca*) contour feather microstructure. *Vestnik Moskovskogo gorodskogo pedagogicheskogo universiteta. Seriya Estestvennyye nauki* [Bulletin of the Moscow City Pedagogical University. Series Natural Sciences], 2011, no. 2, pp. 52–59 (in Russian).
26. Fadeeva E. O. Features of the fine structure of remex of owls (*Strigiformes*), due to the specifics of flight. *Vestnik Moskovskogo gorodskogo pedagogicheskogo universiteta. Seriya Estestvennyye nauki* [Bulletin of the Moscow City Pedagogical University. Series Natural Sciences], 2014, no. 4, pp. 32–38 (in Russian).
27. Fadeeva E. O. Diagnostic possibilities of the birds contour feather on the basis of its microstructure. *Vestnik Moskovskogo gorodskogo pedagogicheskogo universiteta. Seriya Estestvennyye nauki* [Bulletin of the Moscow City Pedagogical University. Series Natural Sciences], 2015, no. 4, pp. 67–77 (in Russian).
28. Fadeeva E. O., Babenko V. G. The diagnostic potential of primary remex microstructure in rare species of falcons (*Falconidae*). *Teoriya i praktika sudebnoi ekspertizy* [Forensic theory and practice], 2017, vol. 12, no. 3, pp. 97–104 (in Russian).
29. Fadeeva E. O. Fine structure of the primary remex of owls (strigiformes). *Zoologicheskii zhurnal* [Zoological journal], 2018, vol. 97, no. 8, pp. 1075–1086 (in Russian).
30. Fadeeva E. O. Microstructure of the Primary Remex of Owls (Strigiformes). *Biology Bulletin*, 2019, vol. 46, no. 7, pp. 780–789. <https://doi.org/10.1134/S1062359019070045>
31. Fadeeva E. O., Babenko V. G. Microstructure of the common barn owl (*Tyto alba* Scopoli, 1769) remex. *Byulleten' Moskovskogo obshchestva ispytatelei prirody. Otdel biologicheskii* [Bulletin of the Moscow Society of Naturalists. Biological department], 2016, vol. 121, no. 6, pp. 18–24 (in Russian).
32. Dickinson E. C. (ed.). *The Howard and Moore Complete Checklist of the Birds of the World. Third Edition*. Princeton, NJ, Princeton University Press, 2003. 1039 p.
33. Verschiedene Federn mit Fahne. *DUDEN Wörterbuch*. Available at: [https://cdn.duden.de/\\_media/\\_full/F/Fahne-201100278768.jpg](https://cdn.duden.de/_media/_full/F/Fahne-201100278768.jpg) (accessed 09.11.2020).
34. Yablokov A. V., Valetskii A. V. Variability of feather structure and egg coloration in some birds. *Zoologicheskii zhurnal* [Zoological journal], 1972, vol. 51, no. 2, pp. 248–258 (in Russian).

35. Kostina G. N., Sokolov V. E., Romanenko E. V., Sidorova T. N., Tarchevskaya V. A., Chernova O. F. Hydrophobic capacity of feather elements in penguins (Aves, Sphenisciformes). *Zoologicheskii zhurnal* [Zoological journal], 1996, vol. 75, no. 2, pp. 237–248 (in Russian).

36. Fadeeva E. O. Fine structure particularities of white-tailed eagles'' (*Haliaeetus albicilla*) primary remexes. *Vestnik Moskovskogo gorodskogo pedagogicheskogo universiteta. Seriya Estestvennye nauki* [Bulletin of the Moscow City Pedagogical University. Series Natural Sciences], 2013, no. 2, pp. 28–36 (in Russian).

37. Fadeeva E. O., Chernova O. F. Peculiarities of the contour feather microstructure in Corvidae family. *Izvestiya Rossiiskoi akademii nauk. Seriya biologicheskaya* [Bulletin of the Russian Academy of Sciences. Biological series], 2011, vol. 4, pp. 436–446 (in Russian).

38. Schmied H. *Die wasserspeichernden Federn der Flughühner (Pteroclididae): Funktionsmorphologie, Benetzungseigenschaften, technischer Nachbau*, 2014. Available at: //hss.ulb.uni-bonn.de/2014/3496/3496.pdf (accessed 09.11.2020).

39. Kartashev N. N. *Systematics of Birds*. Moscow, Vysshaya shkola Publ., 1974. 367 p. (in Russian).

40. Sokolov V. E., Il'ichev V. D. (eds.). *Fauna of the World. Birds*. Moscow, Agropromizdat Publ., 1991. 298 p. (in Russian).

### Информация об авторе

Фадеева Елена Олеговна – канд. биол. наук, доцент, ст. науч. сотрудник. Институт проблем экологии и эволюции им. А. Н. Северцова РАН (Ленинский проспект, 33, 119071, г. Москва, Российская Федерация). E-mail: vgbabenko@gmail.com

### Information about the author

Elena O. Fadeeva – Ph. D. (Biol.), Associate Professor, Senior Researcher. A. N. Severtsov Institute of Ecology and Evolution of the Russian Academy of Sciences (33, Leninsky Prospect, 119071, Moscow, Russian Federation). E-mail: vgbabenko@gmail.com